CHAPTER X

Fluorescent Carbon Nanoparticles

MICHAŁ BARTKOWSKI[a] AND SILVIA GIORDANI[a*]

[a] School of Chemical Sciences, Dublin City University, Glasnevin, Dublin, Ireland

*corresponding email address: silvia.giordani@dcu.ie

Abstract

Fluorescent nanoparticles are indispensable tools often utilised in analytical biology, fluorescence spectroscopy, bioimaging, biophysics, clinical diagnosis, and environmental sensing. Their specific photophysical properties, including brightness, emission wavelength, and analyte sensitivity, can be easily modulated. This affords fluorescent nanoparticles an expansive scope of applicability in imaging and sensing. This chapter gives an overview of various fluorescent carbon nanoparticles, supported by selected literature-case examples, namely on carbon nano-onions, fluorescent carbon dots, and detonation nanodiamonds.

Introduction

Nanoparticles can be crudely defined as 0-dimensional (0D) structures with dimensions below 100 nm[1]. Conversely, *nanomaterials* include nanoparticles and 1D & 2D structures, where 2 or 1 axes, respectively, are below 100 nm in size[2]. For instance, a typical carbon nanotube is a 1D *nanomaterial*; graphene is a 2D *nanomaterial*; and fullerenes are 0D *nanoparticles* / *nanomaterials*. It should also be noted that 3D structures—such as graphite—are not considered nanomaterials, as all axes are over 100 nm in size. Nanoparticles do not have to be spherical—small graphene flakes under 100 nm in size are considered nanoparticles regardless of their planar morphology[3]. Regarding bulk materials, the EU commission defines nanoparticles as those in which at least 50% of the particle size distribution measures under 100 nm[4].

Nanoparticles may possess luminescent properties; particularly, fluorescence. Fluorescence occurs when a molecule absorbs a photon of a specific frequency, which excites a singlet electron in the ground state to a higher electronic state. Subsequently, a photon is emitted as the electron returns to the ground state in a spin-allowed process[5]. The particular characteristics of fluorescence, including the emission wavelength, brightness, and the presence of additional emission bands, may be strongly affected by various chemical and physical factors[6]. These include temperature[7], viscosity[8], pH[9], electric potential[10], tension[11], solvent polarity[12], and the presence of: hydrogen bonds[13], ions[14], quenchers[15] and upconversion agents[16]. By carefully controlling the nanoparticle and these factors, it is possible to achieve fluorescent nanoparticles with desired photophysical properties[17]. For this reason, interest in fluorescent nanoparticles has seen a sharp growth between 2000 and 2014, with an average of 3500 works involving the concept of ‘Fluorescent Nanoparticles’ being published per year since 2014 (see Figure 0.1). Notably, The first time the concept of ‘Fluorescence’ was reported in the literature was by John Frederick William Herschel in 1845[18].

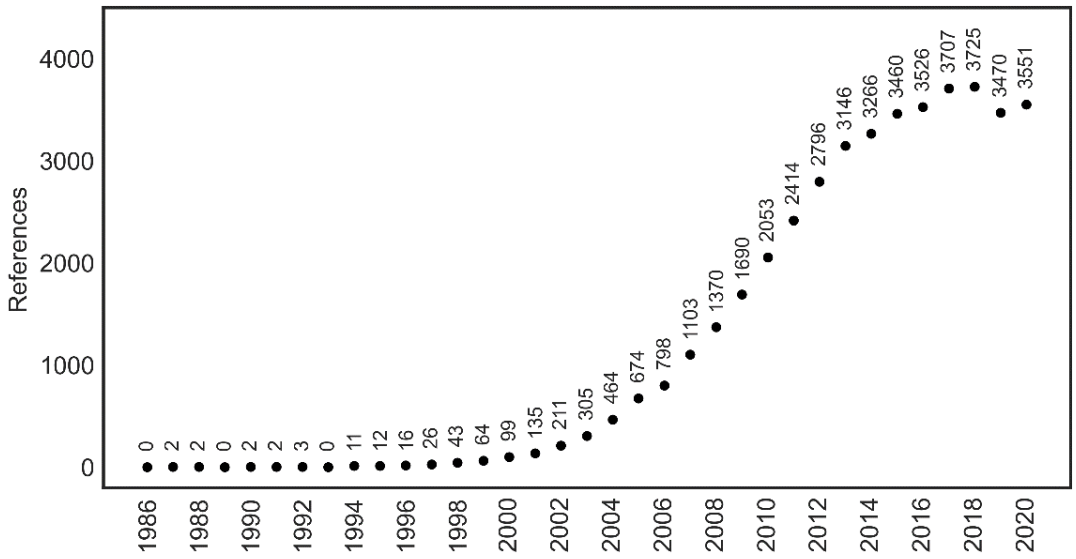

Figure 0.1 Number of publications involving the concept of 'Fluorescent Nanoparticles' between 1986 and 2020 [*Data collected & processed by the author using SciFinder®*]

The two fundamental applicative areas of fluorescent carbon nanoparticles & nanomaterials are imaging & sensing. In 2002, R. Bruce Weisman *et al.* observed that single-walled carbon nanotubes (SWCNTs) exhibit a bright band-gap fluorescence in the NIR region[19,20]. This observation carries deep significance to the fields of bioimaging & biosensing—NIR light can penetrate human tissues, enabling deep-tissue imaging[21,22]. For instance, in 2018, Daniel A. Heller *et al.* utilised the NIR emitting properties of SWCNTs to visualise endolysosomal lipid accumulation in Kupffer cells *in vivo*—a breakthrough in the study of nonalcoholic fatty liver disease, as this is the first method that can do this type of dynamic monitoring without the need for a liver biopsy[23]. This type of bioimaging has been enabled by 'Hyperspectral Microscopy', also developed by the Heller group, which can resolve the NIR fluorescence of CNTs of 17-distinct chiralities (*n*,*m*) (see Figure 0.2)[24].

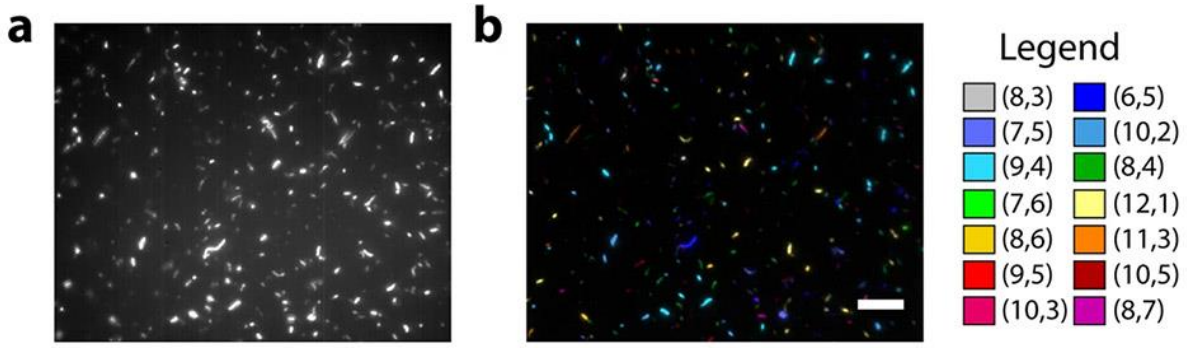

Figure 0.2 A. Hyperspectral microscopy image of CNTs adsorbed onto a glass surface; **B.** false-colour image of A., coloured according to nanotube chirality (*n,m*)[24]; Scalebar = 10 µm. [*Figure adapted from Springer Nature © 2015 under CC BY 4.0 License.*]

Aside from their prevalent use in NIR bioimaging[25–28], fluorescent carbon nanoparticles & nanomaterials have also been utilised in analytical biology[29], fluorescence spectroscopy[30], bioimaging[31], clinical diagnosis[32], biomedical treatment[33], environmental tracing[34], and wastewater treatment[35].

This chapter gives an overview of various fluorescent carbon nanoparticles, supported by selected literature-case examples, namely on carbon nano-onions (CNOs), fluorescent carbon dots and detonation nanodiamonds (DNDs). Numerous reviews offer an exhaustive discussion of various classes of fluorescent nanoparticles[36–38]—these reviews may interest readers looking for a deeper understanding of the different types of fluorescent nanoparticles.

Fluorescent Carbon Nanoparticles

Carbon Nano-onions

First seen by Ugarte in 1992, carbon nano-onions (CNOs) are multi-layered fullerenes composed of concentric shells of sp^2 carbon[39,40]. Many methods are available to prepare CNOs, including arc discharge[41], electron beam irradiation[39], ion implanation[42,43], laser ablation[44], pyrolysis[45], and thermal annealing[46]. These different methods result in CNOs of different shapes, sizes and morphologies. The approach our group utilises for the preparation of CNOs is the thermal annealing of DNDs under an inert He atmosphere. This approach results in small (approx. 5 nm diameter) CNOs of high purity and low polydispersity (see Figure 0.3 A & B)[47]. Notably, the biosafety profile of small CNOs is excellent. Their toxicology has been investigated *in vitro, in vivo* & *ex vivo. In vitro* studies were carried out on HeLa[48] & HeLa Kyoto[49], NIH 3T3[50], MCF-7[51], A2780[52], MDA-MB-231[52], and KB cells[48]. *In vivo* studies

involved *Drosophila melanogaster*[53], *Hydra vulgaris*[54], and *Danio rerio*[55]. *Ex vivo* studies were carried out on murine models[56–58]. In agreement, these studies demonstrate that small CNOs show low systemic toxicity and good biocompatibility. This excellent biosafety profile expands the scope of applicability of small CNOs to the biomedical field. Although CNOs are intrinsically non-luminescent, they are viable scaffolds for coupling with various emitters—desired photoluminescent properties can be imposed on CNOs through the modulation with appropriate fluorophores. Indeed, CNOs have been functionalised with emitters in many instances, thus creating fluorescent nanoparticles capable of emitting from high energy blue light to low energy NIR light. Our group reports using aza-BODIPY & BODIPY derivatives to impart green, red & NIR fluorescence[49,59–64]; fluorescein derivatives to enable green fluorescence[48,56,65,66]; and the tricyclic furo[2,3-*c*]isoquinoline scaffold-based fluorophore to impart deep-blue fluorescence onto CNOs[67].

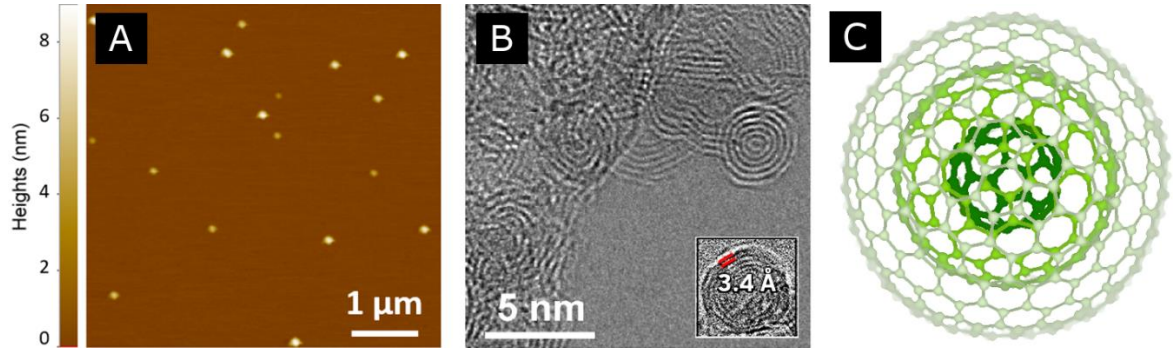

Figure 0.3 A. AFM image of our pristine CNOs (approx. 5 nm in size)[59]; **B.** HRTEM image of our pristine CNOs, Inset: the average interlayer distance[59]; **C.** 3D representation of a 3-layer 2 nm $C_{60}C_{240}C_{500}$ CNO structure. [*Figures A. & B. adapted with permission from RSC*]

In 2014, our group functionalised CNOs with a green-emitting boron dipyrromethane (BODIPY) dye for the first time[59]. The surface of pristine CNOs was covalently functionalised with benzoic acid through a Tour reaction. Subsequently, the BODIPY analogue was covalently attached to the benzoic acid through an EDCl/NHS mediated amidation (see Figure 0.4 1). The emissive properties and high fluorescence afforded to the CNOs by the BODIPY allowed for the systems' utilisation in cellular imaging studies. The BODIPY-CNOs were uptaken by MCF-7 cells. Their uptake and distribution were visualised with confocal microscopy—it was found that BODIPY-CNOs are internalised by endocytosis and predominantly colocalised in the lysosomes after 48 hours. Overall, the low toxicity and high versatility of BODIPY-CNOs have demonstrated their potential as promising fluorescent nanoparticles for theranostic applications[59].

In the same year, we developed a red aza-BODIPY-CNO system. In this approach, an alternative BODIPY analogue (see Figure 0.4 2) was covalently functionalised onto CNOs to afford their NIR fluorescence[49]. The system was utilised for *in vitro* imaging on HeLa Kyoto cells, showing good fluorescence and the systems' distribution in the cytosol. We also demonstrated that pH-induced deprotonation of the -OH group of the aza-BODIPY analogue (see Figure 0.4 2) results in an effective quenching of fluorescence. Consequently, this reversible on/off fluorescence modulation carries the potential for the effective use of this fluorescent nanoparticle in bioimaging and responsive sensing of environmental change.

In an alternative approach, we developed a novel system in which a BODIPY-pyrene derivative was non-covalently attached to the CNO surface (see Figure 0.4 4)[61]—a pyrene moiety facilitated a non-covalent interaction with the pristine CNO surface through π-π stacking. Bioimaging studies and a cytotoxicity assay were performed utilising this system—the system showed good cellular uptake and biocompatibility in HeLa cells. Overall, the successful non-covalent functionalisation of CNOs with the BODIPY derivative highlights the potential of CNOs for the cellular delivery of hydrophobic molecules, including various active pharmaceutical ingridients (APIs)[61].

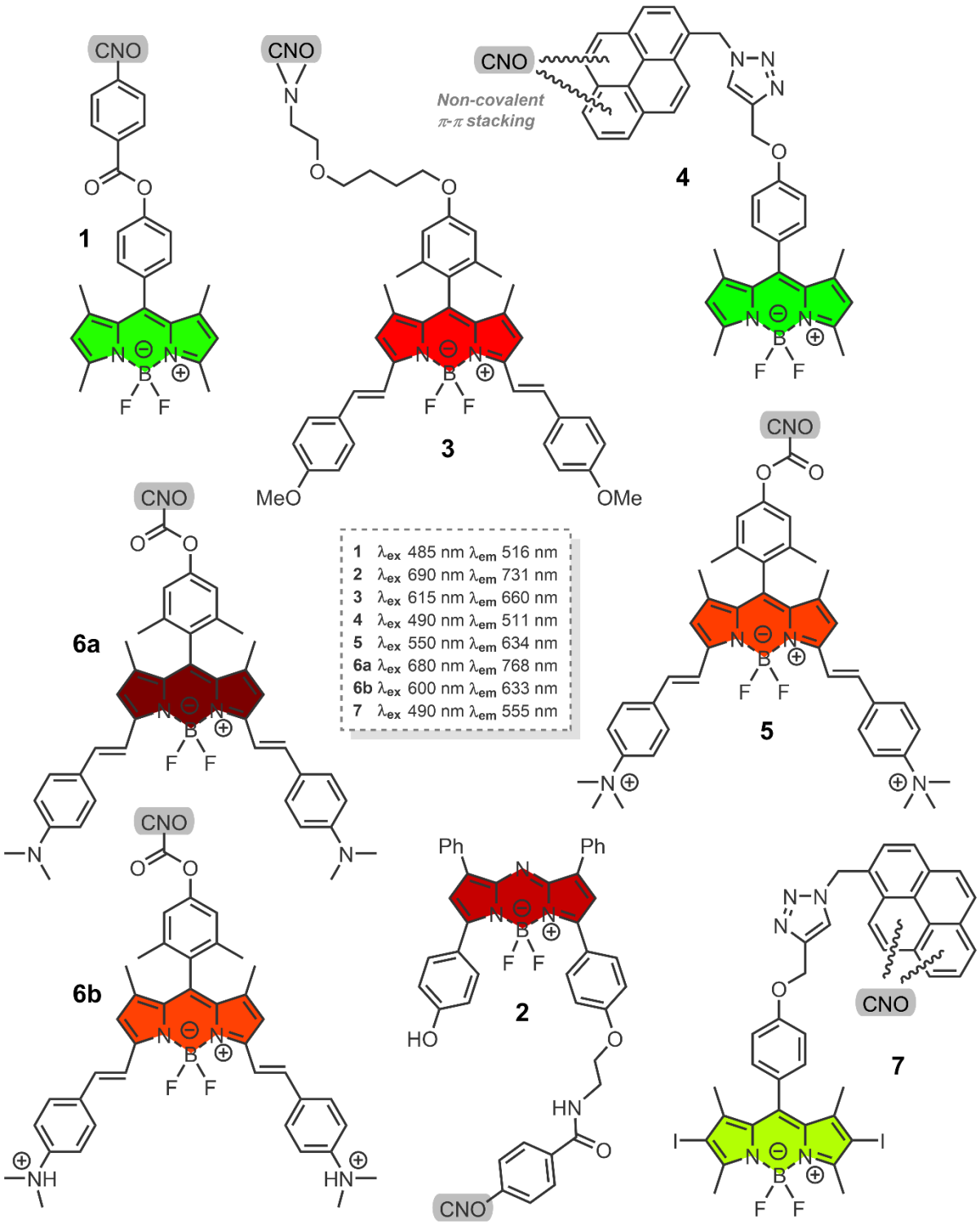

Figure 0.4 The structures of various BODIPY & aza-BODIPY analogues functionalised onto CNOs to create green, red & NIR fluorescent nanoparticles, as developed by our group; **1**[59]; **2**[49]; **3**[60]; **4**[61]; **5**[62]; **6a** & **6b**[63]; **& 7**[64]. The photoexcitation properties (in DMSO) have been tabulated in the centre. The fluorescent core has been coloured according to its emissive wavelength under the specified conditions.

Beyond BODIPY & aza-BODIPY fluorescent CNOs, our group also developed several fluorescein-based CNO systems. In 2015, we covalently surface-functionalised CNOs with fluorescein (see Figure 0.5 1). In our approach, we oxidised DND-derived pristine CNOs. Then, we covalently conjugated the fluorophore through an EDCl/NHS mediated amidation reaction, utilising DMAP as a catalyst. Emission spectroscopy in DMSO confirmed the successful binding of the fluorophore; the CNO-fluorescein nanoparticle had green emission at 518 nm when excited at 490 nm. As a further step in the study, we investigated the system's cellular viability and imaging potential. Cellular viability studies carried out on HeLa cells showed minimal systemic toxicity. Cellular imaging studies, in which confocal micrographs were taken of HeLa cells incubated with the CNO-fluorescein nanoparticles, showed excellent fluorescence and accumulation of the material in the perinuclear region. Furthermore, the system showed increased dispersibility in water—dispersibility is an important aspect for CNMs, which typically suffer from low dispersibility in biocompatible solvents due to their hydrophobic nature[68,69]. Overall, the system showed good potential for biomedical and theranostic applications[65].

In the same year, our group developed another green-fluorescent CNO nanoparticle system[48]. However, in this case, the system was multifuncitonalised with both the green-emitting fluorescein and the targeting agent folic acid. The purpose of the folic acid moiety was to impose targetability onto the system towards cancer cells overexpressing the folate receptor. In this system, the fluorophore was attached to CNOs through a PEG linker to distance the fluorophore from the CNO surface (see Figure 0.5 2); folic acid has been coupled similarly. Overall, this CNO system served its purpose of targeting and imaging cancer cells. The system had excellent brightness, stability and showed rapid, selective uptake in HeLa and KB cancer cell lines, with no significant cytotoxicity[48]. This is an important step towards the utilisation of CNOs as nanocarriers for targeted drug delivery[70].

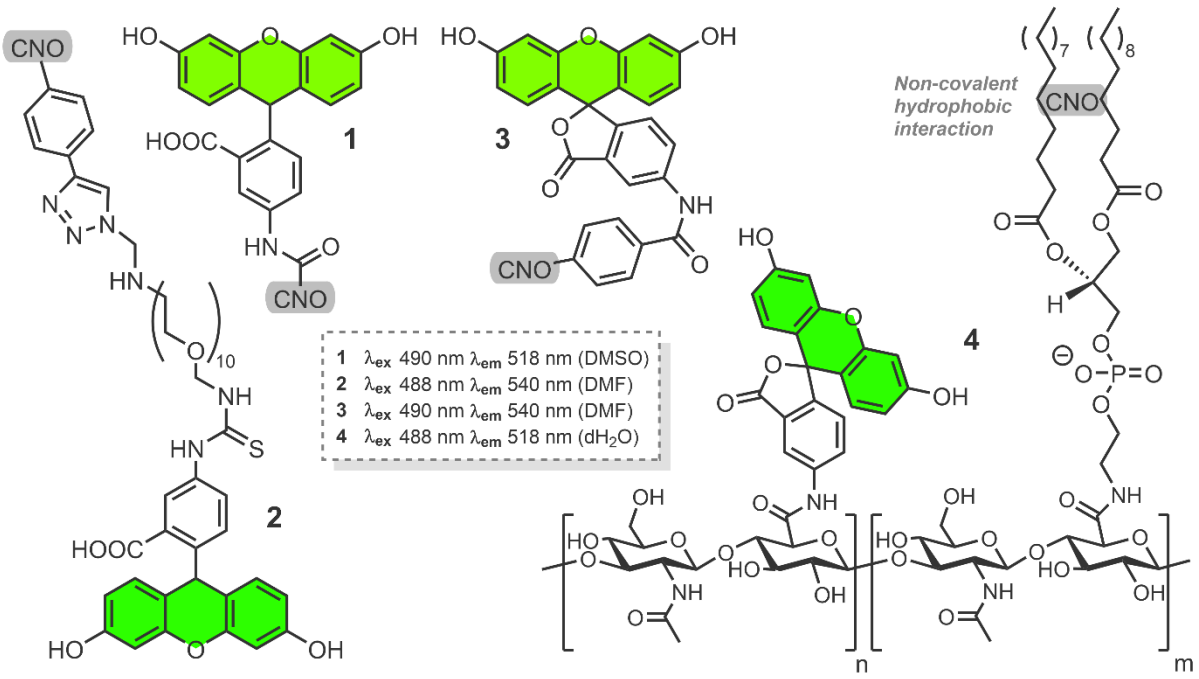

Figure 0.5 The structures of fluorescein-derivative functionalised CNOs developed by our group; **1**[65]; **2**[48]; **3**[56]; & **4**[66]. The photoexcitation properties have been tabulated in the centre. The fluorescent core has been coloured according to its emissive wavelength under the specified conditions.

Although many red & green-emitting CNO systems have been designed to date, it was not until 2020 when the first purely blue light-emitting CNO system was developed. Blue-light emitting fluorophores have been coupled with CNOs to afford their blue-emissive properties[67]. The fluorescent molecules in question were heterocyclic luminophores with a tricyclic furo[2,3-*c*]isoquinoline core (see Figure 0.6), prepared through a multicomponent Ugi reaction and a complex Pd-mediated cascade. The fluorophores were covalently conjugated to surface-oxidised CNOs through an EDCl/NHS mediated amidation. Overall, the three CNO-furo[2,3-*c*]isoquinoline systems showed good deep-blue emissive properties (see Figure 0.6). A 15-20% quenching of fluorescence was observed for the three systems, as attributed to the intrinsic absorptive properties of CNOs. A possible solution to which, as proposed by the authors, is to electronically distance furo[2,3-*c*]isoquinoline from CNOs by introducing a longer linker. Overall, CNOs proved to be a very versatile material of choice for deep-blue emissive nanoparticles. In particular, they were easy to prepare and functionalise, offered excellent stability and a high surface/volume ratio[67].

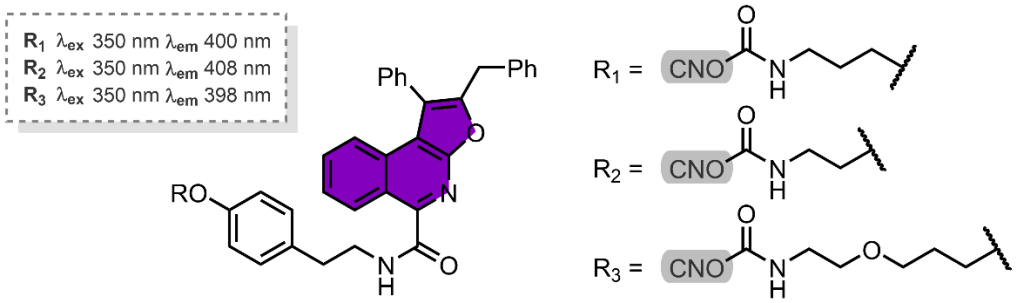

Figure 0.6 The structures of the three CNO-deep-blue emitter dyads reported by Giordani, Riva *et al*. in 2020[67]. The photoexcitation properties (in DMSO) have been tabulated on the left. The fluorescent core has been coloured according to the average (402 nm) of the three derivatives' emissive bands.

Notably, CNOs have been covalently functionalised with other fluorescent probes. In 2010, our group covalently attached a zinc porphyrin to the surface of CNOs through a 1,3 dipolar cycloaddition (*click reaction*)[71]. Photophysical studies of this porphyrin-CNO system indicated that—when excited at 425 nm—two characteristic emission bands are observed; 612 & 662 nm. In a further study of this system, XPS and ToF-SIMS analyses were performed—these techniques confirmed with analytical certainty the successful binding of the fluorescent probe to the CNOs[72].

In summary, fluorescent CNO nanoparticles can be developed through the covalent/non-covalent coupling of the CNM with emitters. And, desired photophysical & emissive properties can be obtained by fine-tuning emitters bonded to the CNO surface. They offer a complimentary choice of fluorescent nanoparticles emissive from the blue to the NIR light range. Typically, green, red & NIR emitting CNOs can be obtained by coupling with BODIPY & aza-BODIPY dyes[49,59–64]; fluorescein-based dyes may afford green fluorescence onto CNOs[48,56,65,66]; and deep-blue emission can be obtained through the coupling with furo[2,3-*c*]isoquinoline fluorophores[67]. Overall, CNOs show good potential as fluorescent nanoparticles of choice for biomedical and theranostic applications, given their excellent biocompatibility, great cellular penetration ability, ease of manipulation, ease of preparation & chemical functionalisation, and high surface/volume ratio[48,51,67,73]. Notwithstanding, their potential extends further—CNOs can act as starting materials for creating other fluorescent nanoparticles. Such examples are described in the *Fluorescent Carbon Dots* section of this chapter, where UV, blue & green-emissive quantum dots have been made from CNOs[74,75].

Fluorescent Carbon Dots

There are many fluorescent nanodot (FND) types, although the difference between them can be blurred due to their overlapping properties. In general, they can be broadly classified into inorganic and *carbon-based* materials. Inorganic FNDs are referred to as semiconductor quantum dots (SQDs), also commonly abbreviated as quantum dots (QDs). Carbon-based FNDs (*Fluorescent Carbon Dots*) consist of three major categories. The first is graphene quantum dots (GQDs), also commonly abbreviated as graphene dots (GDs); the second being carbon quantum dots (CQDs), also commonly abbreviated as carbon dots (CDs); and the final category is carbon nanodots (CNDs) (see Figure 0.7). In their review, Cayuela *et al.* succinctly summarise the properties and characteristics of these four different classifications of FNDs[76]. Briefly, SQDs are composed of inorganic elements, GQDs are composed of carbon, and CQDs & CNDs are composed of carbon with oxygen commonly present. SQDs have a crystalline structure, are spherical and are usually < 6 nm in diameter. Their PL is usually composition-dependent and excitation-independent. GQDs are composed of small discs of single-layer graphite, typically < 20 nm in diameter. Their PL is usually excitation and functionalisation dependent. CQDs are quasi-spherical crystalline materials consisting of mainly sp^2 hybridised carbon, typically < 10 nm in diameter. Their PL is typically excitation- & functionalisation-dependent. Lastly, CNDs are quasi-spherical materials with an amorphous carbon core, typically < 10 nm in diameter. Their PL characteristics are the same as for CQDs[76].

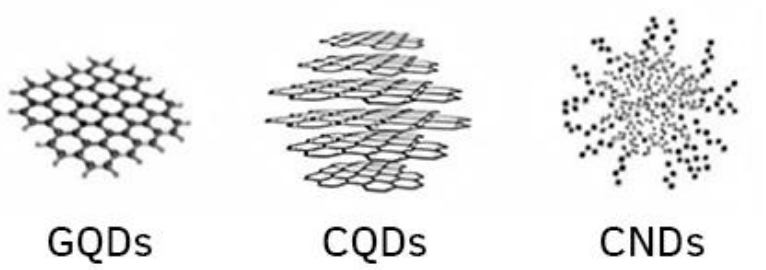

Figure 0.7 The main classes of fluorescent carbon dots[76]. [*Adapted with permission from the RSC.*]

As mentioned in the *Carbon Nano-onions* section, CNOs can serve as a starting material for the preparation of other fluorescent nanoparticles. In 2015, Liu & Kim synthesised UV and blue-emitting graphene quantum dots from DND-derived CNOs[74]. Typically, GQDs are synthesised through a top-down chemical oxidation of various CNMs, including carbon fibres, graphene sheets and carbon black. The authors chose CNOs as their starting material, given their small size and high uniformity/low polydispersity. In choosing CNOs, the authors were able to synthesise GQDs of lower size distribution and more energetically uniform emissive

properties, as compared to what is possible with the aforementioned CNMs. After dialysis and purification, the authors obtained blue-emissive GQDs (λ_{ex} 330 nm; λ_{em} 450 nm) and UV emissive GQDs (λ_{ex} 285 nm; λ_{em} 350 nm). The authors note that, unlike blue/green emissive GQDs, UV emissive GQDs are very rare, especially when prepared using CNMs in a top-down oxidation approach. This underlines the benefit of utilising CNOs as a precursor for the preparation of QDs. The authors speculate that the blue-emissive GQDs originate from the surface of CNOs and that the UV emissive fraction originates from the unoxidised core of CNOs. It was also demonstrated that the blue-emissive GQDs could be used to detect Cu^{2+}, given their ultra-sensitivity to this cation[74].

Similarly, in 2020, our group prepared CDs via a top-down oxidation utilising two CNMs as starting materials[75]; namely, CNOs & GO. The CDs derived from both materials had desirable photoluminescent and physiochemical properties. GO-derived CDs had an excitation-dependant fluorescence, with the strongest excitation bands at 314 & 469 nm, and an emission maxima of 533 nm. Interestingly, the fluorescence of CDs prepared using CNOs was not excitation-dependant, which relates to the surface functional groups of the material. CNO-derived CDs had an emission of 527 nm, with three notable excitation bands; 340, 400 & 460 nm, the latter giving the highest emission. Notably, both CDs showed excellent water dispersibility, with long-term stability[75].

Detonation Nanodiamonds

Detonation nanodiamonds (DNDs) are small (approx. 5 nm) diamond particles (crystallites of sp^3 hybridised carbon; see Figure 0.8) originating from a detonation reaction. Typically, they are produced through the detonation of an oxygen-poor TNT/hexogene mixture[77]. DNDs may have multiple fluorescence sources, including fluorescence originating from defect colour centres[78,79], and from the surface decoration with other emissive species[80,81]. Strictly speaking, the two main types of defect colour centres commonly present in nanodiamonds are nitrogen-vacancy (NV) defects and nitrogen-vacancy-nitrogen (NVN) defects[82,83]. The former is responsible for red/NIR fluorescence, whilst the latter is responsible for the emission of green light. NV & NVN defects have led to various emerging applications of nanodiamonds, ranging from theranostics[84] to nanomagnetometry[82] and nanoscale nuclear magnetic resonance (NMR)[82].

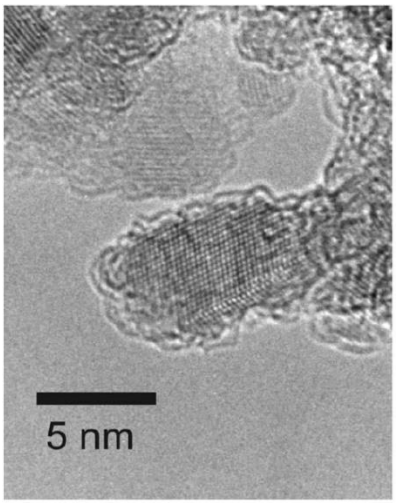

Figure 0.8 HRTEM image of DNDs[85]. [*Adapted with permission from AIP Publishing*]

Similarly to CNOs, the surface of DNDs may also be functionalised with fluorescent moieties; such as carbon dots (CDs). As is the case, in 2018, we investigated CD-functionalised DNDs (CD-DNDs) for their biomedical applications[81]. This was the first investigation of the biological viability of CD-DNDs, as this material has not been previously isolated in high yields. Specifically, the fluorescent nanoparticle utilised in this study consisted of single-digit (4-5 nm) DNDs with surface-bound 1-2 nm CDs composed of sp^2 & amorphous carbon. The CD-DNDs were utilised for *in vitro* bioimaging in MDA-MB-231 breast cancer cells—for which the excitation source was a 488 nm Ar laser, resulting in emission in the 500-550 nm range. Confocal imaging results showed that CD-DNDs are sufficiently luminescent for use in bioimaging studies. Furthermore, an *in vivo* biocompatibility study was carried out using *Danio rerio*. This study showed that the nanoparticles exhibit high biocompatibility and no evident toxic biological consequences in that particular animal model. It should also be noted that—in general—DNDs have low colloidal stability, as is the case with the CD-DND nanoparticles reported in this paper. However, we were able to disperse the CD-DNDs indefinitely by coating them with poly(glycerol). Finally, we speculate that CD-DNDs may be an alternative fluorescent nanoparticle to sub-10 nm DNDs containing NV centres, given their cost-effectiveness, excellent biocompatibility and good luminescence[81].

Conclusion

Fluorescent nanoparticles are very versatile. Their properties extend well beyond their fluorescence, depending on the type of material/particle used. There is a wide array of various intrinsically fluorescent nanoparticles available, with many available commercially. Non-fluorescent nanoparticles can also be functionalised with emissive moieties, thus creating fluorescent nanoparticle-emitter dyads. This coupling can be carried out by covalent means or through non-covalent interactions. This chapter outlined several fluorescent nanoparticles, namely carbon nano-onions (CNOs), fluorescent carbon dots, and detonation nanodiamonds (DNDs). In choosing fluorescent nanoparticles for a given application, their limiting factors need to be considered—these include cytotoxicity, low quantum yield, low dispersibility, and emission outside the biologically transparent NIR optical window. By fine-tuning the nanoparticles, and in certain cases, their surface-bound fluorophores, it is possible to develop fluorescent nanoparticles with desired physiochemical and photoluminescent properties. Such particles are often applied in imaging, sensing, theranostics, and environmental remediation.

ACKNOWLEDGEMENTS

Financial assistance in the form of a Government of Ireland Postgraduate Scholarship (GOIPG) to MB (GOIPG/2019/1820) from the Irish Research Council (IRC) is gratefully acknowledged.

REFERENCES

1 M. Auffan, J. Rose, J.-Y. Bottero, G. V. Lowry, J.-P. Jolivet and M. R. Wiesner, *Nat. Nanotechnol.*, 2009, **4**, 634–641.
2 E. A. J. Bleeker, W. H. de Jong, R. E. Geertsma, M. Groenewold, E. H. W. Heugens, M. Koers-Jacquemijns, D. van de Meent, J. R. Popma, A. G. Rietveld, S. W. P. Wijnhoven, F. R. Cassee and A. G. Oomen, *Regul. Toxicol. Pharmacol.*, 2013, **65**, 119–125.
3 Z. M. Markovic, L. M. Harhaji-Trajkovic, B. M. Todorovic-Markovic, D. P. Kepić, K. M. Arsikin, S. P. Jovanović, A. C. Pantovic, M. D. Dramićanin and V. S. Trajkovic, *Biomaterials*, 2011, **32**, 1121–1129.
4 EU-Commission, *Comm. EEd Bruss. BE*, 2011/696/EU, 2.
5 J. R. Lakowicz, *Principles of Fluorescence Spectroscopy*, Springer Science & Business Media, 2013.
6 A. Chandra, S. Prasad, G. Gigli and L. L. del Mercato, in *Frontiers of Nanoscience*, Elsevier, 2020, vol. 16, pp. 117–149.
7 S. Arai, S.-C. Lee, D. Zhai, M. Suzuki and Y. T. Chang, *Sci. Rep.*, 2014, **4**, 6701.
8 I. López-Duarte, T. Truc Vu, M. Angeles Izquierdo, J. A. Bull and M. K. Kuimova, *Chem. Commun.*, 2014, **50**, 5282–5284.

9 L. Albertazzi, M. Brondi, G. M. Pavan, S. S. Sato, G. Signore, B. Storti, G. M. Ratto and F. Beltram, *PLOS ONE*, 2011, **6**, 28450.
10 T. D. Fehérvári, Y. Okazaki, H. Sawai and T. Yagi, *PLOS ONE*, 2015, **10**, 0133853.
11 A. Colom, E. Derivery, S. Soleimanpour, C. Tomba, M. D. Molin, N. Sakai, M. González-Gaitán, S. Matile and A. Roux, *Nat. Chem.*, 2018, **10**, 1118–1125.
12 J. Yin, M. Peng, Y. Ma, R. Guo and W. Lin, *Chem. Commun.*, 2018, **54**, 12093–12096.
13 K. C. Toh, E. A. Stojković, I. H. M. van Stokkum, K. Moffat and J. T. M. Kennis, *Proc. Natl. Acad. Sci.*, 2010, **107**, 9170–9175.
14 W. Jiang, Q. Fu, H. Fan and W. Wang, *Chem. Commun.*, 2008, 259–261.
15 X. Wang, X. Chen, Z. Xie and X. Wang, *Angew. Chem. Int. Ed.*, 2008, **47**, 7450–7453.
16 G. Yi, Y. Peng and Z. Gao, *Chem. Mater.*, 2011, **23**, 2729–2734.
17 H. Piwoński, T. Michinobu and S. Habuchi, *Nat. Commun.*, 2017, **8**, 15256.
18 J. F. W. Herschel, *Philos. Trans. R. Soc. Lond.*, 1845, **135**, 143–145.
19 M. J. O'Connell, S. M. Bachilo, C. B. Huffman, V. C. Moore, M. S. Strano, E. H. Haroz, K. L. Rialon, P. J. Boul, W. H. Noon, C. Kittrell, J. Ma, R. H. Hauge, R. B. Weisman and R. E. Smalley, *Science*, 2002, **297**, 593–596.
20 D. Movia, E. Del Canto and S. Giordani, *Phys. Status Solidi B*, 2009, **246**, 2704–2707.
21 L. A. Sordillo, Y. Pu, S. Pratavieira, Y. Budansky and R. R. Alfano, *J. Biomed. Opt.*, 2014, **19**, 056004.
22 R. G. Aswathy, Y. Yoshida, T. Maekawa and D. S. Kumar, *Anal. Bioanal. Chem.*, 2010, **397**, 1417–1435.
23 T. V Galassi, P. V Jena, J. Shah, G. Ao, E. Molitor, Y. Bram, A. Frankel, J. Park, J. Jessurun, D. S. Ory, A. Haimovitz-Friedman, D. Roxbury, J. Mittal, M. Zheng, R. E. Schwartz and D. A. Heller, *Sci. Transl. Med.*, 2018, **10**, 2680.
24 D. Roxbury, P. V. Jena, R. M. Williams, B. Enyedi, P. Niethammer, S. Marcet, M. Verhaegen, S. Blais-Ouellette and D. A. Heller, *Sci. Rep.*, 2015, **5**, 14167.
25 K. Soga, K. Tokuzen, K. Tsuji, T. Yamano, H. Hyodo and H. Kishimoto, *Eur. J. Inorg. Chem.*, 2010, 2673–2677.
26 S. K. Yen, D. Jańczewski, J. L. Lakshmi, S. B. Dolmanan, S. Tripathy, V. H. B. Ho, V. Vijayaragavan, A. Hariharan, P. Padmanabhan, K. K. Bhakoo, T. Sudhaharan, S. Ahmed, Y. Zhang and S. Tamil Selvan, *ACS Nano*, 2013, **7**, 6796–6805.
27 T. Ribeiro, S. Raja, A. S. Rodrigues, F. Fernandes, J. P. S. Farinha and C. Baleizão, *RSC Adv.*, 2013, **3**, 9171–9174.
28 Q. Zhao, K. Li, S. Chen, A. Qin, D. Ding, S. Zhang, Y. Liu, B. Liu, J. Zhi Sun and B. Zhong Tang, *J. Mater. Chem.*, 2012, **22**, 15128–15135.
29 J. Liu, X. Yang, X. He, K. Wang, Q. Wang, Q. Guo, H. Shi, J. Huang and X. Huo, *Sci. China Chem.*, 2011, **54**, 1157.
30 B. Kang, M. M. Afifi, L. A. Austin and M. A. El-Sayed, *ACS Nano*, 2013, **7**, 7420–7427.
31 D. Liße, V. Wilkens, C. You, K. Busch and J. Piehler, *Angew. Chem. Int. Ed.*, 2011, **50**, 9352–9355.
32 S. Rogalla, K. Flisikowski, D. Gorpas, A. T. Mayer, T. Flisikowska, M. J. Mandella, X. Ma, K. M. Casey, S. A. Felt, D. Saur, V. Ntziachristos, A. Schnieke, C. H. Contag, S. S. Gambhir and S. Harmsen, *Adv. Funct. Mater.*, 2019, **29**, 1904992.
33 E. S. Glazer and S. A. Curley, *Cancer*, 2010, **116**, 3285–3293.
34 F. Tauro, E. Rapiti, J. F. Al-Sharab, L. Ubertini, S. Grimaldi and M. Porfiri, *J. Nanoparticle Res.*, 2013, **15**, 1884.
35 L. Otero-González, J. A. Field, I. A. C. Calderon, C. A. Aspinwall, F. Shadman, C. Zeng and R. Sierra-Alvarez, *Water Res.*, 2015, **77**, 170–178.
36 O. S. Wolfbeis, *Chem. Soc. Rev.*, 2015, **44**, 4743–4768.
37 M. J. Ruedas-Rama, J. D. Walters, A. Orte and E. A. H. Hall, *Anal. Chim. Acta*, 2012, **751**, 1–23.
38 S. M. Ng, M. Koneswaran and R. Narayanaswamy, *RSC Adv.*, 2016, **6**, 21624–21661.
39 D. Ugarte, *Nature*, 1992, **359**, 707–709.
40 D. Ugarte, *Carbon*, 1995, **33**, 989–993.

41 R. Borgohain, J. Yang, J. P. Selegue and D. Y. Kim, *Carbon*, 2014, **66**, 272–284.
42 T. Cabioc'h, M. Jaouen, E. Thune, P. Gu´erin, C. Fayoux and M. F. Denanot, *Surf Coat Technol*, 2000, **128**, 43–50.
43 E. Thune, T. Cabioc'h, P. Guérin, M. F. Denanot and M. Jaouen, *Mater. Lett.*, 2002, **54**, 222–228.
44 D. Dorobantu, P. M. Bota, I. Boerasu, D. Bojin and M. Enachescu, *Surf. Eng. Appl. Electrochem.*, 2014, **50**, 390–394.
45 S. K. Sonkar, M. Roy, D. G. Babar and S. Sarkar, *Nanoscale*, 2012, **4**, 7670.
46 J. P. Bartolome and A. Fragoso, *Fuller. Nanotub. Carbon Nanostructures*, 2017, **25**, 327–334.
47 M. Bartkowski and S. Giordani, *Nanoscale*, 2020, **12**, 9352–9358.
48 M. Frasconi, R. Marotta, L. Markey, K. Flavin, V. Spampinato, G. Ceccone, L. Echegoyen, E. M. Scanlan and S. Giordani, *Chem. - Eur. J.*, 2015, **21**, 19071.
49 S. Giordani, J. Bartelmess, M. Frasconi, I. Biondi, S. Cheung, M. Grossi, D. Wu, L. Echegoyen and D. F. O'Shea, *J. Mater. Chem. B*, 2014, **2**, 7459–7463.
50 M. d'Amora, V. Maffeis, R. Brescia, D. Barnes, E. Scanlan and S. Giordani, *Nanomaterials*, 2019, **9**, 1069.
51 J. Bartelmess and S. Giordani, *Beilstein J. Nanotechnol.*, 2014, **5**, 1980–1998.
52 M. d'Amora, A. Camisasca, A. Boarino, S. Arpicco and S. Giordani, *Colloids Surf. B Biointerfaces*, 2020, **188**, 110779.
53 M. Ghosh, S. K. Sonkar, M. Saxena and S. Sarkar, *Small*, 2011, **7**, 3170–3177.
54 V. Marchesano, A. Ambrosone, J. Bartelmess, F. Strisciante, A. Tino, L. Echegoyen, C. Tortiglione and S. Giordani, *Nanomaterials*, 2015, **5**, 1331–1350.
55 M. d'Amora, A. Camisasca, S. Lettieri and S. Giordani, *Nanomaterials*, 2017, **7**, 414.
56 M. Yang, K. Flavin, I. Kopf, G. Radics, C. H. A. Hearnden, G. J. McManus, B. Moran, A. Villalta-Cerdas, L. A. Echegoyen, S. Giordani and E. C. Lavelle, *Small*, 2013, **9**, 4194–4206.
57 B. Pakhira, M. Ghosh, A. Allam and S. Sarkar, *RSC Adv.*, 2016, **6**, 29779–29782.
58 M. Trusel, M. Baldrighi, R. Marotta, F. Gatto, M. Pesce, M. Frasconi, T. Catelani, F. Papaleo, P. P. Pompa, R. Tonini and S. Giordani, *ACS Appl. Mater. Interfaces*, 2018, **10**, 16952–16963.
59 J. Bartelmess, E. De Luca, A. Signorelli, M. Baldrighi, M. Becce, R. Brescia, V. Nardone, E. Parisini, L. Echegoyen, P. P. Pompa and S. Giordani, *Nanoscale*, 2014, **6**, 13761–13769.
60 J. Bartelmess, M. Baldrighi, V. Nardone, E. Parisini, D. Buck, L. Echegoyen and S. Giordani, *Chem. - Eur. J.*, 2015, **21**, 9727–9732.
61 J. Bartelmess, M. Frasconi, P. B. Balakrishnan, A. Signorelli, L. Echegoyen, T. Pellegrino and S. Giordani, *RSC Adv.*, 2015, **5**, 50253–50258.
62 S. Lettieri, A. Camisasca, M. D'Amora, A. Diaspro, T. Uchida, Y. Nakajima, K. Yanagisawa, T. Maekawa and S. Giordani, *RSC Adv.*, 2017, **7**, 45676.
63 S. Lettieri, M. d'Amora, A. Camisasca, A. Diaspro and S. Giordani, *Beilstein J. Nanotechnol.*, 2017, **8**, 1878.
64 J. Bartelmess, G. Milcovich, V. Maffeis, M. d'Amora, S. M. Bertozzi and S. Giordani, *Front. Chem.*, 2020, **8**, 573211.
65 M. Frasconi, V. Maffeis, J. Bartelmess, L. Echegoyen and S. Giordani, *Methods Appl. Fluoresc.*, 2015, **3**, 0044005.
66 M. d'Amora, A. Camisasca, A. Boarino, S. Arpicco and S. Giordani, *Colloids Surf. B Biointerfaces*, 2020, **188**, 1100779.
67 V. Maffeis, L. Moni, D. Di Stefano, S. Giordani and R. Riva, *Front. Chem. Sci. Eng.*, 2019, **14**, 76–89.
68 S. Giordani, S. Bergin, V. Nicolosi, S. Lebedkin, W. J. Blau and J. N. Coleman, *Phys. Status Solidi B*, 2006, **243**, 3058–3062.
69 J. C. Zuaznabar-Gardona and A. Fragoso, *J. Mol. Liq.*, 2019, **294**, 111646.
70 M. Bartkowski and S. Giordani, *Dalton Trans.*, 2021, **50**, 2300–2309.
71 K. Flavin, M. N. Chaur, L. Echegoyen and S. Giordani, *Org. Lett.*, 2010, **12**, 840–843.
72 V. Spampinato, G. Ceccone and S. Giordani, *Biointerphases*, 2015, **10**, 19006.
73 M. Bartkowski and S. Giordani, *Nanoscale*, 2020, **12**, 9352.

74 Y. Liu and D. Y. Kim, *Chem. Commun.*, 2015, **51**, 4176–4179.
75 A. Ventrella, A. Camisasca, A. Fontana and S. Giordani, *RSC Adv.*, 2020, **10**, 36404–36412.
76 A. Cayuela, M. L. Soriano, C. Carrillo-Carrión and M. Valcárcel, *Chem. Commun.*, 2016, **52**, 1311–1326.
77 K. Iakoubovskii, M. V. Baidakova, B. H. Wouters, A. Stesmans, G. J. Adriaenssens, A. Ya. Vul' and P. J. Grobet, *Diam. Relat. Mater.*, 2000, **9**, 861–865.
78 A. M. Edmonds, U. F. S. D'Haenens-Johansson, R. J. Cruddace, M. E. Newton, K.-M. C. Fu, C. Santori, R. G. Beausoleil, D. J. Twitchen and M. L. Markham, *Phys. Rev. B*, 2012, **86**, 035201.
79 J. O. Orwa, C. Santori, K. M. C. Fu, B. Gibson, D. Simpson, I. Aharonovich, A. Stacey, A. Cimmino, P. Balog, M. Markham, D. Twitchen, A. D. Greentree, R. G. Beausoleil and S. Prawer, *J. Appl. Phys.*, 2011, **109**, 083530.
80 O. Shenderova, S. Hens, I. Vlasov, S. Turner, Y.-G. Lu, G. Van Tendeloo, A. Schrand, S. A. Burikov and T. A. Dolenko, *Part. Part. Syst. Charact.*, 2014, **31**, 580–590.
81 N. Nunn, M. d'Amora, N. Prabhakar, A. M. Panich, N. Froumin, M. D. Torelli, I. Vlasov, P. Reineck, B. Gibson, J. M. Rosenholm, S. Giordani and O. Shenderova, *Methods Appl. Fluoresc.*, 2018, **6**, 35010.
82 R. Schirhagl, K. Chang, M. Loretz and C. L. Degen, *Annu. Rev. Phys. Chem.*, 2014, **65**, 83–105.
83 M. W. Doherty, N. B. Manson, P. Delaney, F. Jelezko, J. Wrachtrup and L. C. L. Hollenberg, *Phys. Rep.*, 2013, **528**, 1–45.
84 V. Vaijayanthimala, D. K. Lee, S. V. Kim, A. Yen, N. Tsai, D. Ho, H.-C. Chang and O. Shenderova, *Expert Opin. Drug Deliv.*, 2015, **12**, 735–749.
85 S. Tomita, T. Sakurai, H. Ohta, M. Fujii and S. Hayashi, *J. Chem. Phys.*, 2001, **114**, 7477–7482.